Heritage Science

RESEARCH

Open Access

Fracture toughness of aged oil paints

Arkadiusz Janas[1], Nefeli Avgerou[1], Maria N. Charalambides[2], Laura Fuster-López[3] and Łukasz Bratasz[1*]

Abstract

The fracture toughness in opening mode G_{Ic} for selected oil paints from Mecklenburg's Paint Reference Collection after approximately 30 years of natural ageing was determined using the procedure adopted from the ASTM D5528–13 standard in which double cantilever beam specimens are split in tensile tests. The careful reglueing procedure allowed multiple fracturing tests to be carried out that not only improved statistics of the measurements but also provided insight into the variation of the fracture toughness across the paint film observed for some paints. The latter was due to pigment sedimentation or chemical change of the oil binder as a result of the easier access of oxygen from the side open to the air. For the lead white paint, used over centuries both in paint films and oil grounds, the G_{Ic} values more than doubled from 18 to 39 J/m^2 for three consecutive cracks formed at an increasing distance from one side of the paint film. The study demonstrated that fracture toughness corresponding to the first crack formation in aged oil paints ranged between 10 and 40 J/m^2, relatively low values compared to the animal glue-based ground in paintings. In consequence, oil paints are more vulnerable to crack initiation and growth induced by tensile stress than the ground layer. The measurements filled the gap in the knowledge required for the analysis of fracturing or delamination processes in paintings.

Keywords Oil paints, Paint layers, Paintings, Cracking, Fracture properties, Fracture toughness

Introduction

Paintings are in a category of cultural heritage objects that are most valuable but at the same time most vulnerable to relative humidity (RH) variations. Understanding paintings as physical systems is fundamental for their effective preservation, that is to say, for optimizing environmental specifications that would allow museum environments to be effectively managed in terms of reducing energy use and carbon emissions. Paintings are complex multi-layered structures composed usually of wooden or canvas support that was often sized with animal glue, a ground preparatory layer, and paint and varnish layers on the top. All these materials absorb or lose moisture when RH increases or decreases. Changes in the moisture content engender dimensional changes in the paintings' components–swelling or shrinkage. The restraints imposed on these moisture-related dimensional changes, on account of rigid constructions such as frames, stretchers, strainers, or cradles, or a connection to materials that respond differently, induce stresses in all the layers which can cause deformation, cracking, and delamination [1]. Further, shrinkage of the fresh pictorial layer during drying and film-forming processes needs to be taken into account to fully describe the mechanics of paintings [2, 3].

Paintings are often dominant in museum collections and stringent environmental specifications (typically 21 or 22 ± 1 °C) and 50 ± 5% RH) are generally seen as a way to reduce the risk of mechanical damage [4]. The implementation of tight climate control is usually difficult, particularly in historic buildings, and involves energy-intensive air-conditioning systems. Evidence-based, more relaxed environmental specifications [5–7] have been

*Correspondence:
Łukasz Bratasz
lukasz.bratasz@ikifp.edu.pl
[1] Jerzy Haber Institute of Catalysis and Surface Chemistry Polish Academy of Sciences, 30-239 Kraków, Poland
[2] Department of Mechanical Engineering, Imperial College London, London SW7 2AZ, UK
[3] Universitat Politècnica de València, Instituto Universitario de Restauración del Patrimonio, 46022 Valencia, Spain

made possible by studies investigating the moisture and mechanical response of materials and their assemblies, as well as the critical levels of stress/strain at which the materials began to deform plastically or fracture [8–20]. A laminar model of paintings subjected to variations of RH was proposed [1]. It has been assumed that the structural response of a painting is obtained by superimposing individual responses of its components. This simple conceptual model was supported and refined by computer-aided simulations clarifying also a further development of crack systems–the formation of craquelures patterns in the pictorial layers [21–24]. Fracturing in layered materials is due to the stress transfer from the substrate to the uncracked layer or–if cracks are already present–in the area between neighbouring cracks. Stress reaches its maximum value in the middle of the crack-free area. If the strength of the material is exceeded, a new crack nucleates. Ultimately, the crack saturation occurs and an additional load does not initiate new fractures. To summarize, with the use of the described models and simulations of stress fields, tolerable magnitudes of the moisture-induced dimensional changes, and in consequence, tolerable variations of microclimate parameters, have been derived using the criterion of critical stress in the material inducing the strain at break.

The criterion has had its limitations as it refers to an ideal case in which the painting's components are homogenous defect-free materials. In consequence, the criterion cannot be used to estimate the risk of crack formation at defects, or propagation of existing cracks. An alternative approach based on the concepts of fracture mechanics has been used to assess such processes, first proposed by De Willigen twenty years ago for the analysis of craquelures in paintings [25]. The amount of energy released on the crack initiation at a structural flaw in a material or on the propagation of an existing crack is calculated and compared with fracture toughness–the property characterizing a material's ability to resist crack propagation, determined experimentally. It can be interpreted as the energy needed to create a crack of a unit surface area. When the energy release rate exceeds the fracture toughness, crack formation and propagation are assumed. The *J*-integral, proposed by Rice in 1968, is one of the most frequently applied methods to calculate the energy release rate if an elastic behaviour of the material is assumed [26, 27]. In the field of heritage science, the method was used to model the initiation of a crack at a flaw in a ground layer of a painting [22, 24] or to analyse the risk of crack formation and propagation in wooden objects [28].

Although fracture toughness is the fundamental material property in fracture mechanics, it has been determined only for a few materials contained in decorative layers of heritage objects. Schellmann et al. provided fracture toughness for a ground layer used in wooden lacquer objects and for several adhesives used in their conservation [29]. The adhesive fracture energy between alkyd paint and a ground layer with acrylic binder was determined by Tantideeravit et al. [30]. Bratasz et al. determined fracture toughness for animal glue-based ground (gesso) for various pigment-to-binder ratios and RH levels [22]. So far, there has been no data on fracture toughness for paints which hinders the predictive abilities of computational modelling. Eumelen et al. modelled the growth of metal soap crystals in an oil paint layer using a fracture toughness of 416 N/m [31] derived from stress–strain curves for a 14 year-old lead white in cold-pressed linseed oil [32]. Zhang et al. performed a numerical investigation of interfacial and channelling crack growth in an alkyd paint-canvas system using fracture toughness of alkyd paint of 250 N/m [33] determined by Tantideeravit et al. [30]. A similar approach was used by Zhang et al. to evaluate the impact of RH variations on panel paintings. The authors 'reasonably but arbitrarily' assumed the fracture toughness of oil paint to be 25 N/m but performed a parametric analysis varying the parameter in the range of 12.5–50 N/m [34].

The present study has aimed to determine the Mode I fracture toughness of naturally aged oil paints, G_{Ic}. Oil paints are challenging materials as their material parameters are known to evolve over years, even centuries. The study has been made possible by the authors' unique access to samples of dried oil paints currently belonging to Mecklenburg's Paint Reference Collection at the Smithsonian Museum Conservation Institute [35]. The films were cast from 1978/9 until the 1990-ies on polyester sheets. The most recent tensile properties of several paints used in this study were published by Janas et al. [3].

Materials and methods

The oil paint films investigated in this study (Table 1) come from Mecklenburg's Paint Reference Collection at the Smithsonian Museum Conservation Institute and had in their composition a selection of common pigments used throughout history in the production of easel paintings, from traditional (lead white, verdigris, malachite, red ochre, red iron oxide, sap green) to more contemporary (zinc white, synthetic ultramarine). The paints belong to a group of 'control paints' and all were specifically manufactured by Gamblin Artists' Oils Co. with all pigments ground in cold-pressed linseed oil with no other additives. Their compositions expressed as pigment volume concentration PVC = P/(P + B) where P and B are volumes of the pigment and the oil binder, respectively, are provided in Table 1. Both the pigments and the

Table 1 Thickness, pigment volume concentration PVC, and date of casting of oil paint films investigated, all made with cold-pressed linseed oil

Pigments and driers	Thickness [μm]	PVC [%]	Date of casting (dd/mm/yyyy)
Lead white	130	44	07.02.1990
Lead white with litharge	140	44	06.02.1990
Zinc white	260	35	04.12.1998
Titanium white	300	47	07.04.1992
Malachite	290	48	15.03.1990
Sap green	280	–	11.12.1998
Verdigris	420	53	25.01.1999
Raw umber	140	20	02.06.1992
Red iron oxide (1992)	190	12	06.01.1992
Red iron oxide (1998)	250	12	03.12.1998
Synthetic ultramarine	340	45	13.05.1992

oil were purchased from Kremer Pigments Inc. Litharge, a natural mineral form of lead (II) oxide, was added (1.6% w/w) as a drier to one of the paints with lead white. Thin layers of paints were cast in the 1990s on polyester sheets and allowed to dry under controlled environmental conditions of room temperature and the 40–50% RH range until 2005 when they were stored in room conditions with no RH control. A few weeks before the measurements reported in this study, the paint films were carefully peeled off from the polyester sheets by a qualified painting restorer.

The mode I fracture toughness, G_{Ic}, was determined using the procedure adopted from the ASTM D5528–13 standard in which double cantilever beam (DCB) specimens are employed [36]. The DCB specimens were prepared by gluing the paint samples with cyanoacrylate adhesive to the prefabricated mounting elements. The geometry of the DCB specimens was adapted to the size of available oil paint samples: 4 mm wide and 15–20 mm long (Fig. 1). The mounting elements were machined from 4 mm thick polyacrylate sheets to the required geometry. The thickness of the specimen h and the initial crack length a_0 satisfied the criteria of the standard to avoid large deflections of the specimens' arms. After glueing the paint, each DCB specimen was polished from both sides using fine sandpaper to remove the glue residue on the specimen's sides and the edges of the paint film that were penetrated by the glue from the sides. Therefore, the effective specimens' width was approximately 3.8 mm. The exception to the above scheme was one sample with lead white that was 8 mm wide.

As the liquid cyanoacrylate adhesive can potentially penetrate and affect the glued material, the adhesive penetration depth was estimated prior to the test using a HIROX RX1000 microscope. The black colour of the adhesive was easily visible in most paints, particularly the light-coloured ones (Fig. 2). It was found that the glue penetration is around 10–20 μm leaving most of the material unchanged. Prior to the test, each specimen investigated was stored in the laboratory at temperatures ranging between 23 and 25 °C and RH of approximately 40%. A pre-crack in the form of a small V-shape notch 40–50 μm long was introduced in paint using a manually sharpened razor under the microscope.

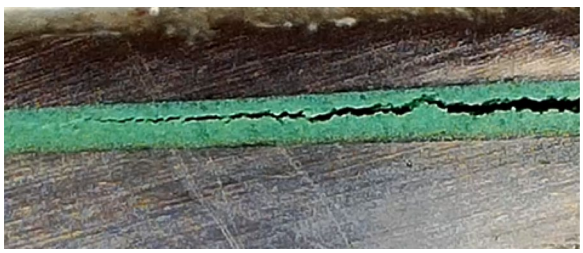

Fig. 2 Microscopic image of a 290 μm thick malachite paint film during the test. Thin dark areas of adhesive penetration are visible at both film surfaces. The crack grew in the paint material not penetrated by the adhesive

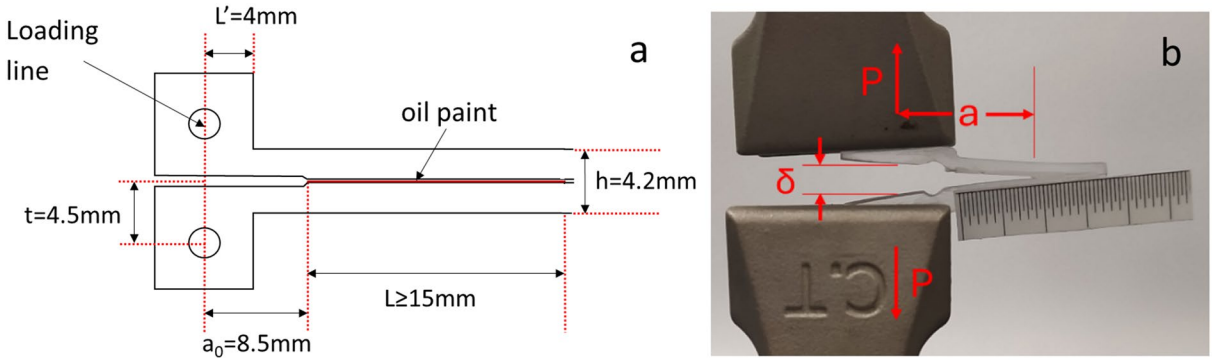

Fig. 1 **a** Geometry of a double cantilever beam specimen, **b** image of the DCB specimen after testing

The fracture toughness experiments were conducted using a Universal Testing Machine (UTM) from Hegewald & Peschke MPT GmbH (Nossen, Germany) equipped with a video microscope DTX 500 Levenhuk (Tampa, USA), manually translated to follow and record the position of the crack tip. A printed scale with a graduation of 1 mm was attached to one side of the DCB specimen allowing the crack length to be measured (Fig. 1b). The synchronization of the recorded video with the UTM was obtained by the manual pressing of the DCB specimen before and after the test.

The DCB specimens were mounted on the UTM using steel loading pins inserted into the holes in the mounting elements and load was applied by moving the upper crosshead at a rate of 0.0625 mm/min. Due to the limited amount of the paint material available for the tests, between one and three replicate samples for each material were tested (Table 2).

Some tested samples, where the crack ran cohesively inside the paint layer, were re-glued and tested again using the same testing procedures. This allowed variation of the fracture toughness across the films to be determined. Due to polishing of the specimens' sides after reglueing, the specimens' width gradually decreased. Approximately each polishing reduced the specimen's width by 100 µm. The procedure was repeated until reglueing was impossible for one of two reasons: reglueing the sample several times caused complete penetration of the paint by the glue, or the rough surface of the developed crack made reglueing impossible. Figure 3 illustrates the lead white sample split three times during the consecutive loading cycles. For most of the paints, the crack initiated in the paint that was not penetrated by the adhesive. When the crack grew in the paint penetrated by the adhesive, the results were discarded, and the regluing procedure was terminated. The total number of tests on each material is given in Table 2.

Table 2 Number of oil paint samples investigated as well as number of repeated tests on the same sample

Paint	Number of samples	Number of tests on a single sample
Lead white	2	3;1
Lead white with litharge	2	1;1
Zinc white	3	1;3;1
Titanium white	1	1
Malachite	1	2
Sap green	1	5
Verdigris	1	6
Raw umber	1	1
Red iron oxide (1998)	1	1
Red iron oxide (1990)	1	1
Synthetic ultramarine	1	1

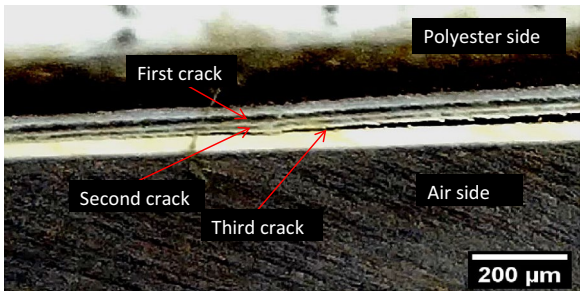

Fig. 3 Microscopic image of the paint with lead white after the third test. The spaces in the first and the second cracks were filled with the glue. The third crack is open

The applied load, P, load point displacement, δ, and crack length, a, (Fig. 1), recorded in each test, were used to calculate fracture toughness G_{Ic} applying the Modified Beam Theory (MBT) Method as described in the ASTM D5528–13 standard:

$$G_{Ic} = \frac{3P\delta}{2b(a+|\Delta|)} \cdot \frac{F}{N}$$

where b is the specimen width. Δ, F, and N correct for the beam not being perfectly built-in at the crack tip, for large displacements, and the stiffening effect of the end-blocks, respectively. Their values were calculated as defined in the standard.

Results and discussion

Two load–displacement curves recorded in the tests for paints with verdigris and lead white are shown, as examples, in Fig. 4. After the initial, almost linear, part of the curve, a small or large drop in load is recorded (curves a and b, respectively) reflecting the onset of crack propagation to a few millimetres beyond the pre-crack in the specimen. It was assumed that a crack with a sharp tip was created in this initial process. The load and displacement values were subsequently recorded at every 1 mm increment of crack growth as they reflected stable propagation of a crack until the sample failed. For each test, an average fracture toughness G_{Ic} was calculated using the propagation values. For each paint, fracture toughness was calculated as an average of G_{Ic} values from all tests performed–single or multiple after the reglueing procedure, except for single tests. The average, minimum, and maximum G_{Ic} values for the paints tested are presented in Table 3. In all the tests, the fracture path propagated through the paint layer either along the midplane or closer to the paint film surface that was cast on the

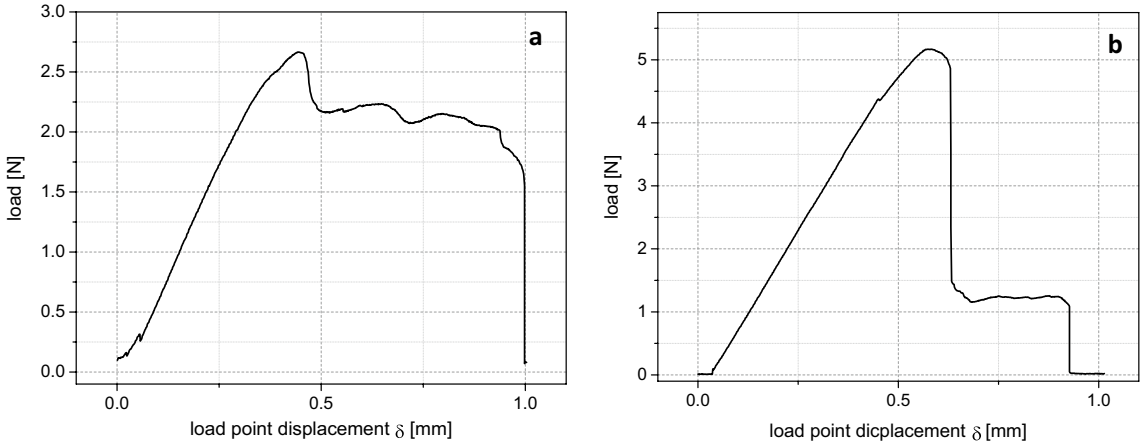

Fig. 4 Stable and unstable fracture of the DCB specimens with paints: **a** verdigris, **b** lead white

Table 3 Fracture toughness G_{Ic} of the oil paints investigated

Paint	Drying time [year]	G_{Ic} [J/m^2]	Min–Max G_{Ic} [J/m^2]	Location of crack propagation
Lead white	33	28	18–39	Close to the polyester sheet substrate
Lead white with litharge	33	12	10–13	
Zinc white	25	17	7–25	
Verdigris	23	22	9–32	
Sap green	25	83	31–180	Complex pattern
Titanium white	31	22	–	At the midplane
Malachite	33	35	33–37	
Raw umber	31	15	–	
Red iron oxide (1998)	24	17	–	
Red iron oxide (1992)	31	40	–	
Synthetic ultramarine	31	36	–	

polyester sheet substrate. Only the paint with sap green experienced a complex fracturing pattern described in the text. The locations of crack propagation are indicated in Table 3.

The observed variability in the measurements indicates that dried oil paints are not homogenous materials. The reason for the large variability is the inhomogeneity of the paint across the film. For paint with lead white, G_{Ic} values more than doubled from 18 to 39 J/m^2 for three consecutive cracks, visible in Fig. 3, formed at an increasing distance from the side that was initially cast on the polyester sheet. Similarly, in six tests performed on the same sample of paint with verdigris, the G_{Ic} values were by two standard deviations lower (approx. 9 J/m^2) close to the side cast on the polyester sheet than from the free side (approx. 31 J/m^2). This effect resulted from an increase of the pigment-volume concentration PVC at the polyester side caused by pigment sedimentation in paints, as made evident by a SEM micrographs for the verdigris paint [37]. A decreasing amount of the oil binder (high PVC), caused by the sedimentation, led to a decrease in the bonding area between pigments and, in consequence, to a decrease in the cohesive energy of the stratum. The same tendency was documented for gesso whose fracture toughness started to decrease above the PVC of approximately 91% whereas practically no bonding was observed for PVC exceeding 95% [22]. In turn, the inhomogeneity across the film of paint with sap green resulted from the chemical change of the oil binder due to easier access of the oxygen from the film side open to the air. A difference in colour between the 'air' and 'polyester' sides was apparent: the paint was yellowish from the air side and green from the polyester side. Although no chemical analysis was carried out on the sample, oxidative processes rather than light damage must have led to the colour change as all samples were stored in dark conditions. The interface between the two zones

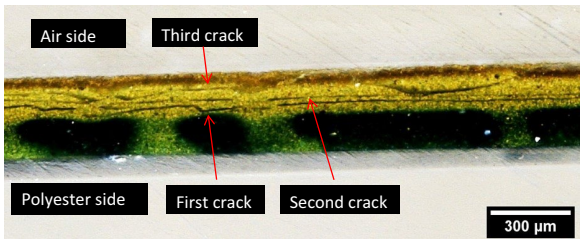

Fig. 5 Microscopic image of the paint with sap green after the third test indicating the propagation levels of consecutive cracks

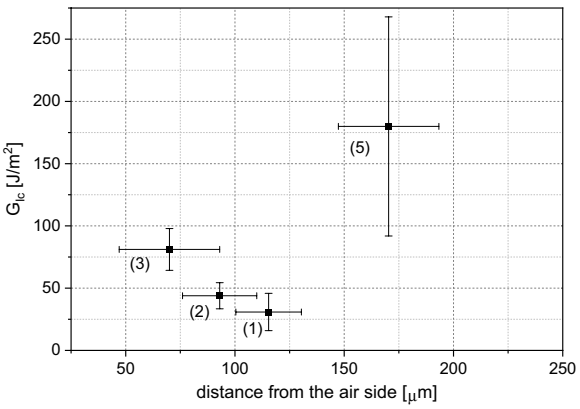

Fig. 6 G_{Ic} values determined for cracks in sap green paint determined at various depths as measured from the air side. The numbers in brackets indicate the consecutive loading cycles in the DCB test

was an obvious flaw in the paint layer structure as the first crack developed at this interface (Fig. 5) and the G_{Ic} value was the lowest of all measured (Fig. 6). The second and third cracks developed sequentially closer to the air side. The fourth crack developed at the interface between the paint and the cyanoacrylate adhesive and, therefore, was disregarded. Finally, the fifth developed in the green part, close to the polyester side and the calculation revealed the highest G_{Ic} of all measured (Fig. 6).

The only paint allowing for analysis of the evolution of fracture toughness with age was red iron oxide. A more than twofold increase in fracture toughness was observed for 31-year-old red iron oxide paint compared to 24-year-old paint which points to the progressing molecular evolution of the oil binder even after 25 years. The iron oxide-based pigments are known to induce hydrolysis reactions degrading the binder in oil paints which experience decreasing stiffness and increasing plasticity during the initial curing period [38]. However, similarly to the evolution of fracture toughness, an increase in stiffness is observed in the paint containing iron oxide cured for 31 years [3].

Conclusions

The reported measurements have confirmed the outcome of earlier studies that a fracture mechanics approach can be used to characterize components of the pictorial layers in paintings. The modified double cantilever beam method allowed the fracture toughness in opening mode to be successfully determined even for small sizes of available valuable oil paint films naturally aged for approximately 30 years.

The general conclusion from the study is that aged oil paints have low values of the first-crack fracture toughness between 10 J/m^2 and 40 J/m^2, compared to the animal glue-based ground in paintings for which fracture toughness is approximately 100 J/m^2 [22] as well as to alkyd paints for which the value is 250 J/m^2 [30]. This demonstrates that paints are more vulnerable to crack initiation and growth induced by tensile stress than the glue-based ground layer. The values determined generally agree with those assumed by Zhang et al. [34] and used for the evaluation of the impact of RH variations on panel paintings but are approximately one order of magnitude lower than the value used by Eumelen et al. [31] in the simulation of cracking of paint layer induced by the growth of metal soap crystals. Furthermore, aged oil paints may exhibit varying fracture toughness across their thickness owing to changing PVC caused by pigment sedimentation or to chemical change of the oil binder due to easier access of the oxygen from the side open to the air. Low values of fracture toughness determined for the initial crack propagation in paints with lead white and verdigris are particularly striking. The observed heterogeneity across the paint film is particularly relevant for research on paints with lead white. The latter is a pigment that is frequently studied owing to its widespread use over centuries both in paint films and oil grounds. Though the effect of heterogeneity needs further investigation, the lowest levels of fracture toughness determined in this study should be used when analysing the process of delamination of the paints with lead white.

The values reported in this study fill the gap in the literature on material properties of aged components of the pictorial layers and are a further step in understanding paintings as physical systems. In particular, they allow more accurate modelling and understanding of the mechanisms of crack formation at a structural flaw, the propagation of existing cracks, also leading to delamination and flaking of the layers, or metal-soap protrusions in oil-based pictorial layers.

Undoubtedly, the presented research is only a starting point in characterizing the ageing of oil paints. As demonstrated in the earlier studies referenced in this paper, the properties of oil paints evolved over decades or centuries. Oil paints become stiffer and more brittle but

the information about the detailed evolution of fracture toughness with age still needs to be investigated.

Abbreviations

DCB	Double cantilever beam
PVC	Pigment volume concentration
RH	Relative humidity
UTM	Universal testing machine
w/w	Weight per weight

Acknowledgements
The authors thank Roman Kozłowski (the Jerzy Haber Institute of Catalysis and Surface Chemistry Polish Academy of Sciences) for his assistance in the interpretation of the results and correcting the manuscript.

Author contributions
ŁB conceived the research hypotheses, AJ, ŁB, MNC planned research methods and experiments, LFL prepared the specimens, AJ and NA carried out the measurements, AJ, ŁB, MC analysed and interpreted results, ŁB wrote the first draft of the manuscript. All authors discussed the research outcome, as well as developed and approved the final manuscript.

Funding
The research leading to these results has received funding from the Norwegian Financial Mechanism 2014–2021, project registration number 2019/34/H/HS2/00581, and the statutory research fund of the Jerzy Haber Institute of Catalysis and Surface Chemistry Polish Academy of Sciences. Laura Fuster Lopez's work was financed by the PID2019-106616 GB-100 project granted by MCIN/AEI/https://doi.org/10.13039/501100011033.

Availability of data and materials
All data needed to evaluate the conclusions in the paper are presented in the paper. Additional data related to this paper may be requested from the corresponding author.

Declarations

Competing interests
The authors declare that they have no competing interests.

Received: 30 December 2023 Accepted: 21 March 2024
Published online: 28 March 2024

References

1. Mecklenburg MF. Determining the acceptable ranges of RH and T in museums and galleries, Part 1. A report of the Museum Conservation Institute, the Smithsonian Institution. 2011. http://www.si.edu/mci/english/learn_more/publications/reports.html. Accessed 29 December 2023.
2. Krzemień L, Łukomski M, Bratasz Ł, Kozłowski R, Mecklenburg MF. Mechanism of craquelure pattern formation on panel paintings. Stud Conserv. 2016;61:324–30.
3. Janas A, Mecklenburg MF, Fuster-López L, Kozłowski R, Kékicheff P, Favier D, Krarup Andersen C, Scharff M, Bratasz Ł. Shrinkage and mechanical properties of drying oil paints. Herit Sci. 2022;10:181.
4. Thomson G. The Museum Environment. 2nd ed. London: Butterworths-Heinemann; 1986.
5. Michalski S. Climate guidelines for heritage collections: where we are in 2014 and how we got here. In: Stauderman S, Tompkins WG, editors. Proceedings of the Smithsonian Institution Summit on Museum Preservation Environment. Washington DC: Smithsonian Institution Scholarly Press; 2016. p. 7–32.
6. Bickersteth J. IIC and ICOM-CC 2014 declaration on environmental guidelines. Stud Conserv. 2016;61:12–7.
7. Museums, Galleries, Archives and Libraries. ASHRAE Handbook, Chap. 24. Peachtree Corners: American Society of Heating and Air-Conditioning Engineers; 2019.
8. Mecklenburg MF, Tumosa CS, Erhardt D. Structural response of painted wood surfaces to changes in ambient relative humidity. In: Dorge V, Howlett FC, editors. Painted wood: history and conservation. Los Angeles: The Getty Conservation Institute; 1998. p. 464–83.
9. Rachwał B, Bratasz Ł, Krzemień L, Łukomski M, Kozłowski R. Fatigue damage of the gesso layer in panel paintings subjected to changing climate conditions. Strain. 2012;48:474–81.
10. Hagan EWS. Thermo-mechanical properties of white oil and acrylic artist paints. Prog Org Coat. 2017;104:28–33.
11. Luimes RA, Sukier ASJ, Verhoosel CV, Jorissen AJM, Schellen HL. Fracture behaviour of historic and new oak wood. Wood Sci Technol. 2018;52:1243–69.
12. Janas A, Fuster-López L, Krarup Andersen C, Escuder AV, Kozłowski R, Poznańska K, Gajda A, Scharff M, Bratasz Ł. Mechanical properties and moisture-related dimensional change of canvas paintings–canvas and glue sizing. Herit Sci. 2022;10:160.
13. Bridarolli A, Freeman AA, Fujisawa N, Łukomski L. Mechanical properties of mammalian and fish glues over range of temperature and humidity. J Cult Herit. 2022;53:226–35.
14. Poznańska K, Hola A, Kozłowski R, Strojecki M, Bratasz Ł. Mechanical and moisture-related properties of dried tempera paints. Herit Sci. 2024;12:25.
15. Hedley G. Relative humidity and the stress/strain response of canvas paintings: uniaxial measurements of naturally aged samples. Stud Conserv. 1988;33:133–48.
16. Andersen CK. Lined canvas paintings. Mechanical properties and structural response to fluctuating relative humidity, exemplified by the collection of Danish Golden Age paintings at Statens Museum for Kunst. Thesis. KADK Royal Danish Academy of Fine Arts; 2013.
17. Andersen CK, Mecklenburg MF, Scharff M, Wadum J. With the best intentions. Wax-resin lining of Danish Golden Age paintings (early 19th century) on canvas and changed response to RH. In: Bridgland J, editor. ICOM Committee for Conservation 14th Triennial Conference, Melbourne, 15–19 September 2014, preprints, 14; 2014.
18. Lee DS, Kim N, Scharff M, Nielsen AV, Mecklenburg MF, Fuster-López L, Bratasz Ł, Andersen CK. Numerical modelling of mechanical degradation of canvas paintings under desiccation. Herit Sci. 2022; 10: 130.
19. Bratasz Ł, Łukomski M, Klisińska-Kopacz A, Zawadzki W, Dzierżęga K, Bartosik M, Sobczyk J, Lennard FJ, Kozłowski R. Risk of climate-induced damage in historic textiles. Strain. 2015;51:78–88.
20. Krzemień L, Czyżewska A, Soboń M, Kozłowski R, Bratasz Ł. Risk of climate-induced damage in historic parchment. Herit Sci. 2020;8:17.
21. Bosco E, Suiker ASJ, Fleck NA. Moisture-induced cracking in a flexural bilayer with application to historical paintings. Theor Appl Fract Mech. 2021;112: 102779.
22. Bratasz Ł, Akoglu KG, Kékicheff P. Fracture saturation in paintings makes them less vulnerable to environmental variations in museums. Herit Sci. 2020;8:11.
23. Jamalabadi MYA, Zabari N, Bratasz Ł. Three-dimensional numerical and experimental study of fracture saturation in panel paintings. Wood Sci Technol. 2021;55:1555–76.
24. Antropov S., Bratasz Ł. Development of craquelure patterns in paintings on panels. Herit Sci. 2024;12:89.
25. De Willigen PA. Mathematical study on craquelure and other mechanical damage in paintings. Delft: Delft University Press; 1999.
26. Rice JR. A path independent integral and the approximate analysis of strain concentration by notches and cracks. J Appl Mech. 1968;35:379–86.
27. Anderson TL. Fracture mechanics fundamentals and application. New York: Taylor and Francis; 2005.
28. Soboń M, Bratasz Ł. A method for risk of fracture analysis in massive wooden cultural heritage objects due to dynamic environmental variations. Eur J Wood Wood Prod. 2022;80:1201–13.
29. Schellmann NC, Taylor AC. Establishing the fracture properties of delaminating multi-layered decorative coatings on wood and their changes after consolidation with polymer formulations. J Mat Sci. 2015;50:2666–81.
30. Tantideeravit S, Charalambides MN, Balint DS, Young CRT. Prediction of delamination in multilayer artist paints under low amplitude fatigue loading. Eng Fract Mech. 2013;112–113:41–57.
31. Eumelen GJAM, Bosco E, Suiker ASJ, Hermans JJ, van Loon A, Keune K, Iedema PD. Computational modelling of metal soap formation in historical oil paintings: the influence of fatty acid concentration and nucleus

geometry on the induced chemo-mechanical damage. SN Appl Sci. 2020. https://doi.org/10.1007/s42452-020-3038-z.
32. Mecklenburg MF, Tumosa CS, Erhardt D. The changing mechanical properties of aging oil paints. In: Vandiver PB, Mass JL, Murray A, editors. Materials Issues in Art and Archaeology, VII, Materials Research Society, 2004; 852:13–24.
33. Zhang R, Wood JD, Young CRT, Taylor AC, Balint DS, Charalambides MNA. Numerical investigation of interfacial and channelling crack growth rates under low-cycle fatigue in bi-layer materials relevant to cultural heritage. J Cult Herit. 2021;49:70–8.
34. Zhang R, Taylor AC, Charalambides MN, Balint DS, Young CRT, Barbera D, Blades N. A numerical model for predicting the time for crack initiation in wood panel paintings under low-cycle environmentally induced fatigue. J Cult Herit. 2023;61:23–31.
35. Mecklenburg MF, Tumosa CS. An introduction into the mechanical behavior of paintings under rapid loading conditions. In: Art in transit: studies in the transport of paintings. Washington D.C: National Gallery of Art; 1991. p. 137–71.
36. ASTM D5528–13, Standard test method for mode I Interlaminar fracture toughness of unidirectional fiber-reinforced polymer matrix composites, ASTM International, West Conshohocken, PA; 2013.
37. Bridarolli A, Łukomski M. Upublished study. The Getty Conservation Institute, Los Angeles; 2023.
38. Mecklenburg MF, Tumosa CS, Vicenzi EP. The influence of pigments and ion migration on the durability of drying oil and alkyd paints. In: Mecklenburg MF, Charola AE, Koestler RJ, editors. New insights into the cleaning of paintings, proceedings from the Cleaning 2010 International Conference, Universidad Politécnica de Valencia and Museum Conservation Institute. Washington D.C.: Smithsonian Institution Scholarly Press; 2013. p. 59–67.

Publisher's Note